Effects of Amino Acid Chirality and the Chemical Linker on the Cell Permeation Characteristics of Cyclic Prodrugs of Opioid Peptides

Bianca M. Liederer, Tarra Fuchs, David Vander Velde, Teruna J. Siahaan, and Ronald T. Borchardt*

Department of Pharmaceutical Chemistry, The University of Kansas, Lawrence, Kansas 66047

Received March 28, 2005

Previously, our laboratory showed that the oxymethyl-modified coumarinic acid (OMCA) cyclic prodrug of the opioid peptide DADLE ([D-Ala^2,D-Leu^5]-Enk, H-Tyr-D-Ala-Gly-Phe-D-Leu-OH) exhibited low permeation across both the intestinal mucosa and the blood−brain barrier (BBB). This low cell permeation arose from its strong substrate activity for efflux transporters in these biological barriers. In an attempt to determine whether the chirality of the amino acid asymmetric centers could influence the solution structure of the cyclic prodrugs and thus their substrate activities for efflux transporters, we synthesized cyclic prodrugs of the opioid peptides H-Tyr-Ala-Gly-Phe-D-Leu-OH ([Ala^2,D-Leu^5]-Enk), H-Tyr-D-Ala-Gly-Phe-Leu-OH ([D-Ala^2,Leu^5]-Enk), and H-Tyr-Ala-Gly-Phe-Leu-OH ([Ala^2,Leu^5]-Enk). In an attempt to determine whether the chemical linker (OMCA) bestowed efflux substrate activity on the cyclic prodrugs, we synthesized capped linear derivatives (acetylated on the N-terminal and amidated on the C-terminal end) of [Ala^2,D-Leu^5]-Enk, [D-Ala^2,Leu^5]-Enk, and [Ala^2,Leu^5]-Enk. The solution conformations of the cyclic prodrugs were determined by molecular dynamics simulations using two-dimensional NMR data. The physicochemical properties (molecular surface area, polar surface area, and cLogP) were estimated computationally using Sybyl. Cell permeation characteristics were assessed using Caco-2 cells in the presence and absence of known inhibitors of efflux transporters. Despite apparent differences in their solution conformations and their physicochemical properties, the cyclic prodrugs of DADLE, [Ala^2,D-Leu^5]-Enk, [D-Ala^2,Leu^5]-Enk, and [Ala^2,Leu^5]-Enk all exhibited strong substrate activity for efflux transporters in Caco-2 cells. In contrast, the capped linear derivatives of [Ala^2,D-Leu^5]-Enk, [D-Ala^2,Leu^5]-Enk, and [Ala^2,Leu^5]-Enk exhibited very poor substrate activity for efflux transporters in Caco-2 cells. Therefore, the substrate activities of the cyclic prodrugs for efflux transporters in Caco-2 cells and in the intestinal mucosa and the BBB in vivo are most likely due to the chemical linker used to prepare these molecules and/or its effect on solution structures of the prodrugs.

Introduction

Opioid peptides such as DADLE ([D-Ala^2,D-Leu^5]-enkephalin, H-Tyr-D-Ala-Gly-Phe-D-Leu-OH) have poor intestinal mucosal and blood−brain barrier (BBB) permeability because they are paracellular permeants.[1] Therefore, their potential therapeutic effects cannot be exploited clinically.[2] To achieve better membrane permeation, opioid peptides must possess physicochemical properties that allow them to diffuse across cellular barriers (e.g., intestinal mucosa and BBB) via the transcellular pathway rather than the paracellular pathway and not be substrates for efflux transporters.[3−6]

One possible approach to solving this drug delivery problem involves cyclization of opioid peptides using chemical linkers.[7,8] These chemical linkers can be designed to be susceptible to esterase hydrolysis, leading to a cascade of chemical reactions that result in the eventual release of the peptide.[9] Using this prodrug strategy, opioid peptides can be converted from paracellular to transcellular permeants.[10−12] For example, oxymethyl-modified coumarinic acid (OMCA)-DADLE (**1a**), a cyclic prodrug of DADLE that was developed earlier in our laboratory, exhibited significantly better intrinsic cell permeation characteristics than the parent linear peptide, DADLE, itself.[10−12] However, despite its favorable physicochemical properties for transcellular permeation, OMCA-DADLE (**1a**) showed low permeation across both the intestinal mucosa and the BBB, which could be attributed to its substrate activity for efflux transporters, mainly MDR1 and MRP2.[9,10,13]

a) Cyclic Prodrugs

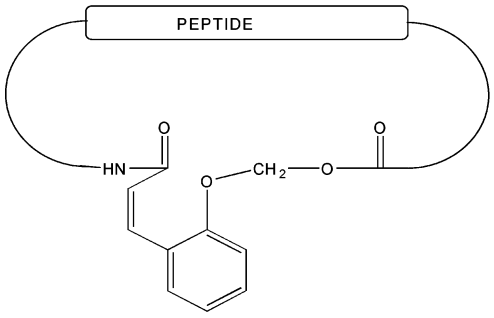

Cyclic Prodrug	Peptide
1a	Tyr-D-Ala-Gly-Phe-D-Leu (DADLE)
1b	Tyr-Ala-Gly-Phe-D-Leu ([Ala^2,D-Leu^5]-Enk)
1c	Tyr-D-Ala-Gly-Phe-Leu ([D-Ala^2,Leu^5]-Enk)
1d	Tyr-Ala-Gly-Phe-Leu ([Ala^2,Leu^5]-Enk)

b) N-Acetylated and C-Amidated Derivatives

2a	Ac-Tyr-Ala-Gly-Phe-D-Leu-NH_2 (Ac-[Ala^2,D-Leu^5]-Enk-NH_2)
2b	Ac-Tyr-D-Ala-Gly-Phe-Leu-NH_2 (Ac-[D-Ala^2,Leu^5]-Enk-NH_2)
2c	Ac-Tyr-Ala-Gly-Phe-Leu-NH_2 (Ac-[Ala^2,Leu^5]-Enk-NH_2)

Figure 1. Structures of OMCA cyclic opioid prodrugs **1a**−**d** and N-acetylated and C-amidated derivatives of linear opioid peptides **2a**−**c**.

* To whom correspondence should be addressed. Phone: (785) 864-3427. Fax: (785) 864-5736. E-mail: rborchardt@ku.edu.

10.1021/jm050277f CCC: $33.50
Published on Web 02/02/2006

Scheme 1

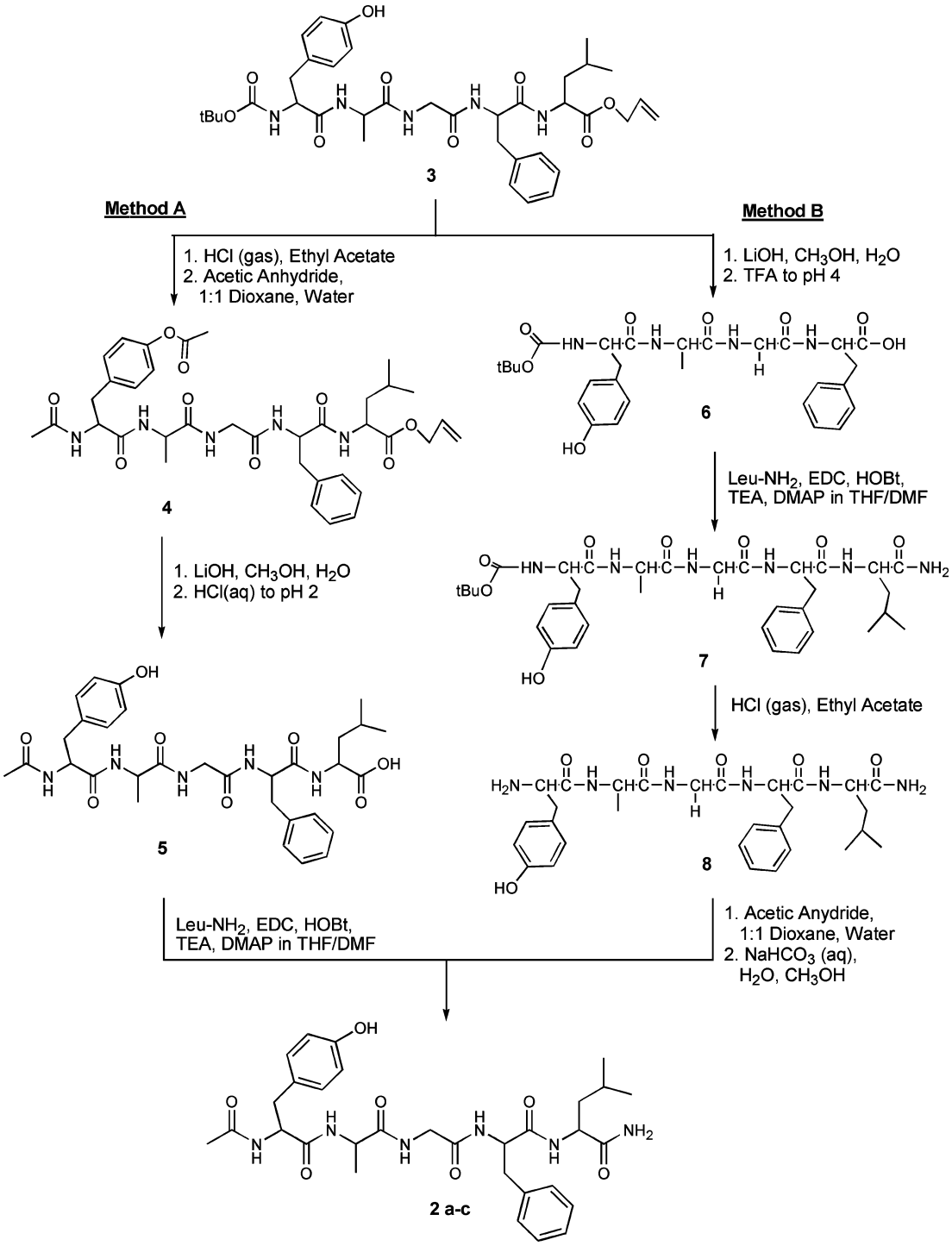

The chirality of the amino acids in an opioid peptide like DADLE can be manipulated while still retaining pharmacological activity.[14−16] For instance, it has been reported that the residues in positions 2 and 5 of enkephalins, e.g., [Leu^5]-Enk (H-Tyr-Gly-Gly-Phe-Leu-OH) and [Met^5]-Enk (H-Tyr-Gly-Gly-Phe-Met-OH), are not critical for receptor binding interactions. Consequently, analogues of these compounds including DADLE, [Ala^2,D-Leu^5]-Enk (H-Tyr-Ala-Gly-Phe-D-Leu-OH), [D-Ala^2,Leu^5]-Enk (H-Tyr-D-Ala-Gly-Phe-Leu-OH), and [Ala^2,-Leu^5]-Enk (H-Tyr-Ala-Gly-Phe-Leu-OH) are biologically active although they vary in their potencies.[14−16] Since DADLE, [Ala^2,D-Leu^5]-Enk, [D-Ala^2,Leu^5]-Enk, and [Ala^2,Leu^5]-Enk are diastereomers, they would be expected to exhibit different physicochemical properties. Similarily, cyclic prodrugs of these opioid peptides might also be expected to have different physicochemical characteristics.

Physicochemical factors, including polar surface area characteristics, high hydrogen-bonding potential, and flexibility, have all been shown to influence the ability of a molecule to permeate cell membranes.[3−5] For instance, as the polar surface area or hydrogen-bonding potential of a transcellular permeant increases, its cell membrane permeation will decrease. Thus, changes in the chirality of the Ala and/or Leu residues in the peptide portion of cyclic prodrugs could alter these physicochemical properties and thus influence their passive diffusion across cell membranes.[3,17]

Polar surface characteristics are also very important for the binding of molecules to efflux transporters.[18−24] It has been

shown that a particular arrangement of electron donor groups in the molecule is essential for substrate recognition by P-gp. Again, altering the chirality of the Ala and/or Leu residues in DADLE or in the cyclic prodrug of the opioid peptides could change their polar surface area characteristics and, therefore, affect their ability to interact with efflux transporters.

In an attempt to determine how the chirality of Leu and Ala in the opioid peptide affects its solution conformation, physicochemical properties, and cell permeation characteristics, we synthesized cyclic prodrugs of the opioid peptides [Ala^2,D-Leu^5]-Enk, [D-Ala^2,Leu^5]-Enk, and [Ala^2,Leu^5]-Enk (Figure 1, **1b**−**d**) and compared these to the properties of OMCA-DADLE (**1a**), which had been reported earlier by our laboratory.[8,10] Additionally, capped derivatives (acetylated on the N-terminal and amidated on the C-terminal end) (Scheme 1) of [Ala^2,D-Leu^5]-Enk (**2a**), [D-Ala^2,Leu^5]-Enk (**2b**), and [Ala^2,Leu^5]-Enk (**2c**) were synthesized and their cell permeation characteristics determined in an attempt to elucidate whether the chemical linker itself or conformations induced by the linker were inducing the substrate activity for efflux transporters.

Results and Discussion

Synthesis. The N-acetylated, C-amidated peptides **2a**−**c** were synthesized using solution-phase methodologies[8] beginning with the tetrapeptide Boc-Tyr-(D,L)-Ala-Gly-Phe-OAll (**3**) (Scheme 1). Method A involved the Boc-deprotection of the tetrapeptide (**3**), followed by acetylation of the N-terminal end (as well as the Tyr phenol), deprotection of the C-terminal carboxylic group (as well as the Tyr phenol), and, finally, coupling of the D-Leu-amide or L-Leu-amide to Ac-Tyr-Ala-Gly-Phe-OH (**5**) to yield Ac-[Ala^2,D-Leu^5]-Enk-NH$_2$ (**2a**) and Ac-[Ala^2,Leu^5]-Enk-NH$_2$ (**2c**), respectively. Method B involved initial deprotection of the carboxylic acid of Boc-Tyr-D-Ala-Gly-Phe-OAll (**3**) using LiOH.[25] The resulting Boc-protected peptide, Boc-Tyr-D-Ala-Gly-Phe-OH (**6**), was then coupled with Leu-amide. After Boc-deprotection, acylation of the Tyr-D-Ala-Gly-Phe-Leu-NH$_2$ (**8**) yielded the desired Ac-[D-Ala^2,Leu^5]-Enk-NH$_2$ (**2b**).

Conformational Characteristics. 1. NMR Spectroscopy. NMR studies were performed to determine whether changes in the chirality of the Ala or Leu amino acid residues of the opioid peptide changed the solution conformations and, therefore, the hydrogen-bonding interactions, polar surface characteristics, and other physicochemical characteristics of the resulting cyclic prodrugs **1b**−**d** compared to **1a**. These conformational/physicochemical changes could then impact the intrinsic permeation of the cyclic prodrugs via the transcellular pathway.[3,26,27] Furthermore, these changes could affect the interaction of the cyclic prodrugs with the efflux transporters that limit their intestinal and BBB permeation.[18−24] The populated conformations can be expected to vary with the nature of the environment, from the very polar environment of water to the lipophilic interior of the cell membrane. For these purposes, the most relevant environment is the zone of reduced polarity at the water−membrane interface. The slow step in transcellular diffusion is likely to be entry into the membrane from this point, because of the high energy cost of breaking hydrogen bonds with water molecules. Evidence for intramolecular hydrogen bonds in the peptide backbone is of particular interest, because if these supplant hydrogen bonds with water, it could lower the energy cost of desolvation.[28,29] Although the membrane surface environment is sometimes modeled in NMR experiments by detergent micelles in water, these cyclic peptides were insufficiently soluble in water for such experiments. As an alternative, a mixture of dimethyl sulfoxide (DMSO) and water (4:1 v/v) was used instead, which dissolved the peptides in concentrations suitable for the NMR experiments. The conformational results we report for this solvent mixture will not necessarily hold for water, but we have no experimental results in water to make the comparison.

Table 1. Chemical Shifts, Coupling Constants, and Dihedral Angles (Calculated from Coupling Constants and Measured from Energy-Minimized Average Structures) for Cyclic Prodrugs **1b**−**d**

	chemical shift (ppm) NH	coupling constant $^3J_{NH\alpha}$ (Hz)	calcd ϕ (deg)	measured ϕ (deg)	measured ψ (deg)
OMCA-[Ala^2,D-Leu^5]-Enk (**1b**)					
Tyr-1	7.94	5.7	−168, −60, 20, 120	114	−132
Ala-2	8.32	5	172, −67, 31, 103	−69	−50
Gly-3[a]	8.07	11	−135, −54, 54, 135	−88	41
Phe-4	7.36	7.5	−157, −80, 35, 90	−150	−57
D-Leu-5	8.42	7.1	161, 79, −30, −91	101	NA
OMCA-[D-Ala^2,Leu^5]-Enk (**1c**)					
Tyr-1	8.47	5.5	−170, −71, 22, 97	−96	108
D-Ala-2	8.66	4.6	175, 63, −18, −108	−27	−77
Gly-3[a]	8.00	11	−135, −54, 54, 135	−89	55
Phe-4	7.55	7.9	−157, −83, 35 to 90	−160	−71
Leu-5	8.32	7.2	−160, −78, 33, 90	−153	NA
OMCA-[Ala^2,Leu^5]-Enk (**1d**)					
Tyr-1	7.10	2	−48, −2, 123, 155	117	112
Ala-2	8.48	2.3	−50, 0, 120, 160	71	−56
Gly-3[a]	8.36	12	−128, −60, 60, 128	−162	−72
Phe-4	7.70	8.7	−175, −63, 18, 108	−72	−35
Leu-5	8.62	5.8	−165, −57, 23, 118	−85	NA

[a] $\sum J_{NH-CH2}$.

The proton chemical shifts of **1b**−**d** were determined using 2D ^{1}H−^{1}H-correlation spectroscopy (COSY), 2D ^{1}H−^{1}H homonuclear Hartmann−Hahn (HOHAHA), and 2D ^{1}H−^{1}H rotating frame Overhauser effect spectroscopy (ROESY) (Table 1). The amide−amide correlations in the ROESY are the most important peaks in terms of understanding the peptide backbone conformation and intramolecular hydrogen bonding.

Like all cyclic peptides, these compounds must formally reverse the direction of the peptide backbone twice, but the chain reversal may or may not take place in a normal β-turn conformation. In all three cyclic peptides, ROE cross-peaks were observed between the NH of Gly and the NH of Phe, and also between the NH of Phe and the NH of Leu/D-Leu (Figure 2). These through-space interactions are the expected markers for a type I β-turn structure.[30] Although in both **1b** and **1d** the β-turn occurred at exactly the same residues (i.e., Ala, Gly, Phe, and Leu), the first connectivity (Gly 3-Phe 4) was much stronger than the second (Phe 4-Leu 5) for OMCA-[Ala^2,Leu^5]-Enk (**1d**), while the reverse was true for OMCA-[Ala^2,D-Leu^5]-Enk (**1b**). In two of the three compounds, a third cross-peak was also seen, between Ala 2 and Gly 3; this is strongest in **1c**, weaker in **1b**, and absent entirely in **1d**. This third cross-peak would not be observed in a normal type I β-turn and is indicative of varying amounts of distortion away from typical β-turn geometry. A long string of consecutive amide−amide cross-peaks is more characteristic of an α-helix, but a conformation in α-space would also have a series of low (∼4 Hz) coupling constants ($^3J_{HN\alpha}$),[30] which was not observed. It is unlikely that a short cyclic peptide like **1c** could adopt such an α-helix structure in any case. It can also be appreciated from Figure 2 and Table 1 that the chemical shifts of the amide protons vary significantly across the series. A fourth related compound, the cyclic prodrug of DADLE (**1a**), displayed no amide−amide cross-peaks at all and thus adopts a very different nonstandard secondary structure. These NMR data clearly show that changes in the stereochem-

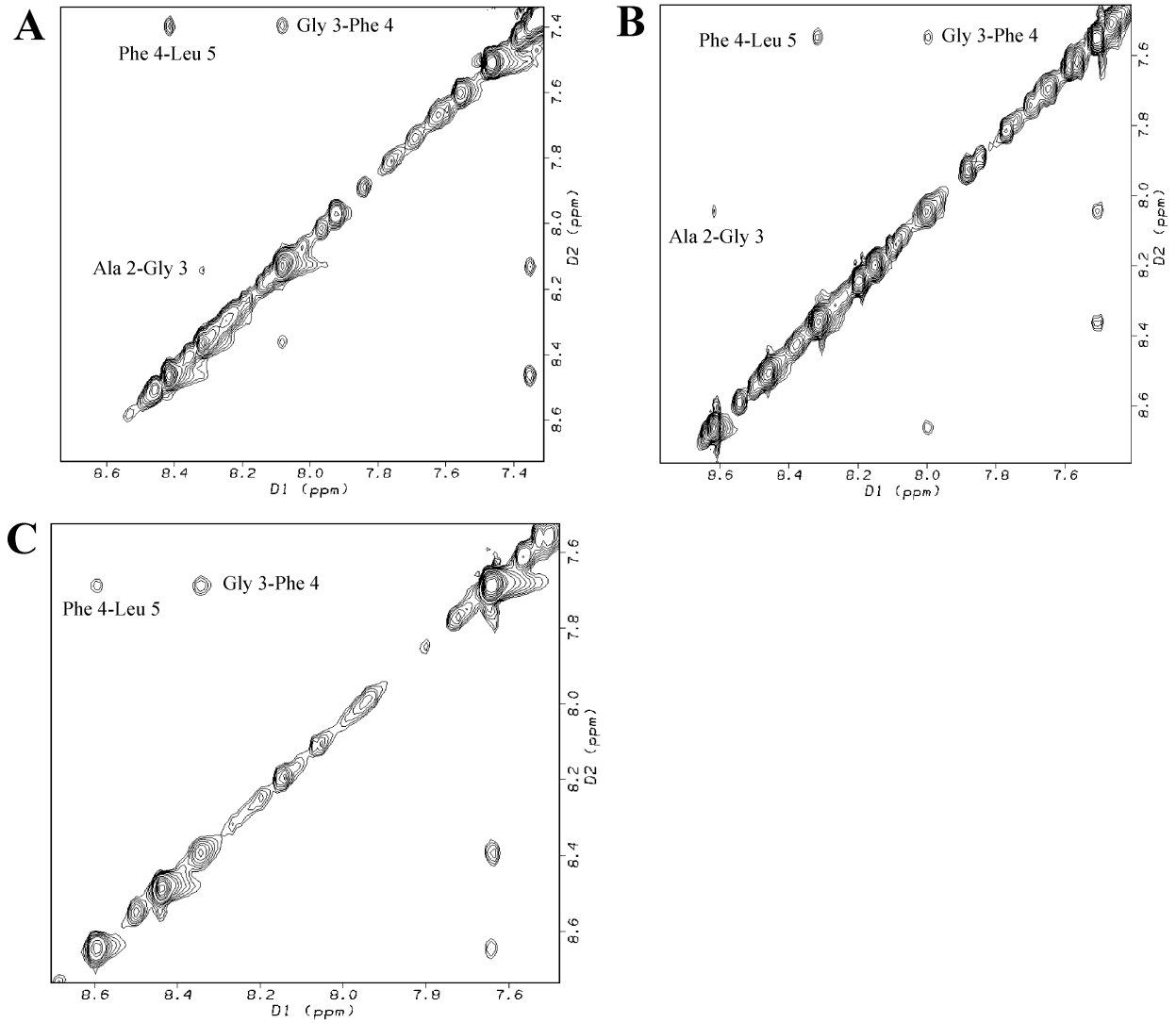

Figure 2. Amide region of the ROESY spectrum of the cyclic prodrugs OMCA-[Ala^2,D-Leu^5]-Enk **1b** (A), OMCA-[D-Ala^2,Leu^5]-Enk **1c** (B), and OMCA-[Ala^2,Leu^5]-Enk **1d** (C).

istry of the Ala and Leu residue in DADLE can dramatically alter the conformations of corresponding cyclic prodrugs.

On the basis of the large flexibility and, therefore, random structure of short linear peptides, no NMR studies or MD simulations were pursued for the capped linear opioid peptides **2a**−**c**.[26,31]

2. Molecular Dynamics (MD) Simulations. To further elucidate the solution conformations of cyclic prodrugs **1b**−**d**, MD simulations were done using distance constraints obtained from the ROESY experiments described above.

The final energy-minimized average solution structures are shown in Figure 3A−C. All dihedral angles (ϕ) of the residues of these average solution structures except for Ala-2 in OMCA-[Ala^2,Leu^5]-Enk (**1d**) are within 35° of those ϕ angles calculated from the NMR coupling constant data (Table 1). Moreover, most measured distances are consistent with the ROE distance constraints. Cyclization represents a powerful constraint on the accessible peptide backbone conformations for these molecules, but little or no constraint on side chain conformations. Side chain−backbone and side chain−side chain ROE's were minimal, e.g., compared with what is observed for a protein, and overall there is little data to suggest preferred side chain conformations are present. The side chains are represented in Figure 3, but unlike the backbone conformation, the side chain conformations shown only represent one low energy possibility.

All solution structures of cyclic prodrugs **1b**−**d** appeared to be stabilized at different locations by two to three intramolecular hydrogen bonds involving mainly the backbone of the peptides. These types of intramolecular hydrogen bonds would reduce the extent to which these functional groups hydrogen bond intermolecularly with water. Consequently, less desolvation energy would be required for the molecules to enter and diffuse across lipophilic cell membranes by the transcellular pathway. The correlation of decreased hydrogen bonding potential of peptides to increased permeability across Caco-2 cells has been demonstrated previously and found to be the main driving force for transcellular diffusion.[28,29] The hydrogen bonds shown were produced during the simulations, and they were not added as constraints prior to the simulations.

In our simulations, OMCA-[Ala^2,Leu^5]-Enk (**1d**) displayed a hydrogen bond between the NH of Gly and C═O of Tyr and between the NH of Tyr and C═O of Leu. In contrast, OMCA-[Ala^2,D-Leu^5]-Enk (**1b**) showed a hydrogen bond between the NH of Leu and C═O of Tyr and between the NH of Tyr and the phenolic oxygen of the promoiety. For OMCA-[D-Ala^2,-Leu^5]-Enk (**1c**) three hydrogen bonds were observed, i.e., between the NH of Phe and C═O of Ala, the NH of Tyr and C═O of Leu, and the NH of Leu and C═O of Tyr. For OMCA-DADLE (**1a**) two possible hydrogen bonds have been reported involving the NH of Gly and the oxygen of the phenol group

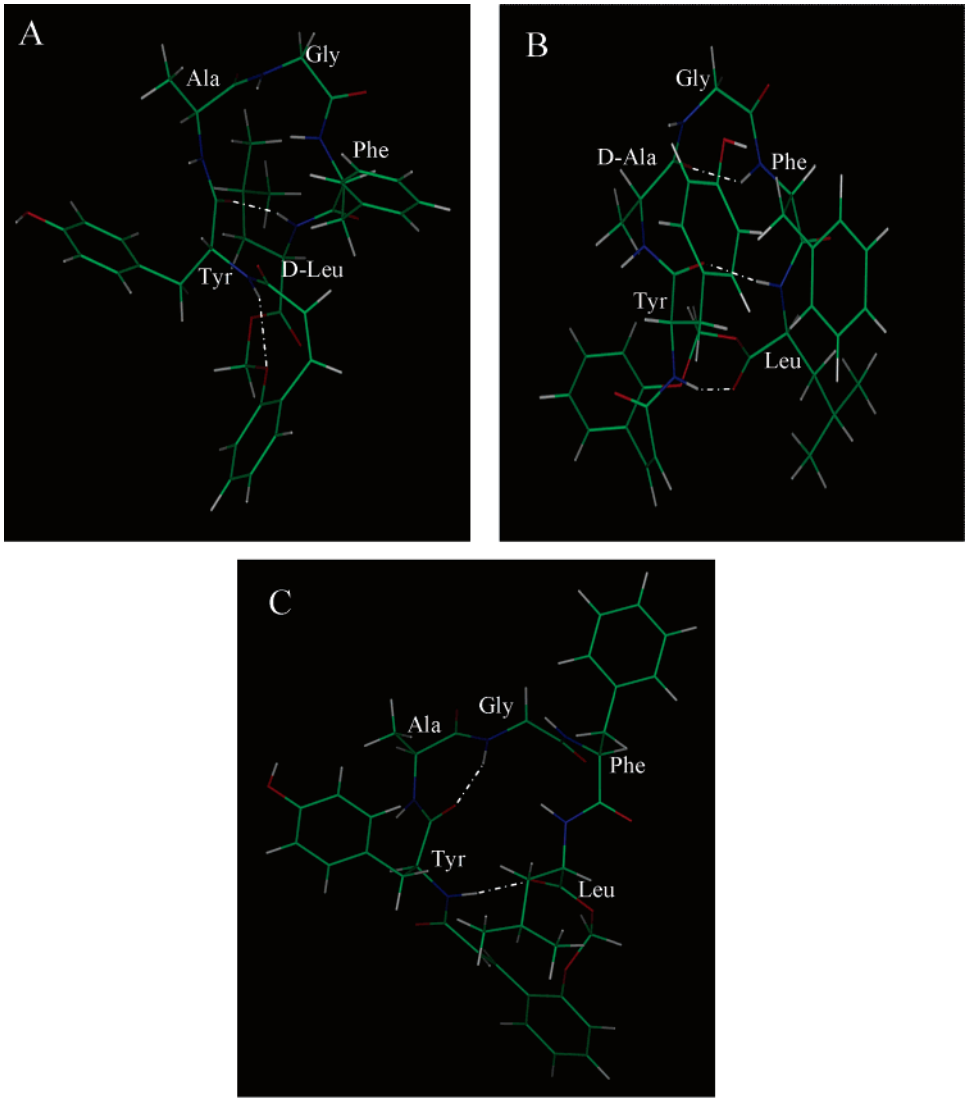

Figure 3. Energy-minimized average solution structures of the cyclic prodrugs (A) OMCA-[Ala^2,D-Leu^5]-Enk **1b**, (B) OMCA-[D-Ala^2,Leu^5]-Enk **1c**, and (C) OMCA-[Ala^2,Leu^5]-Enk **1d**; (− · −) intramolecular hydrogen bond.

Table 2. Calculated Physicochemical Properties of Cyclic Prodrugs **1a**−**d**

	OMCA-DADLE **1a**	OMCA-[Ala^2,D-Leu^5]-Enk **1b**	OMCA-[D-Ala^2,Leu^5]-Enk **1c**	OMCA-[Ala^2,Leu^5]-Enk **1d**
cLogP	5.4	5.4	5.4	5.4
molecular surface area (Å^2)	571	589	560	650
polar surface area (Å^2)	170	139	150	150
polar surface area (% of the total molecular surface area)	30	24	27	23

Table 3. Calculated Physicochemical Properties of the Capped Linear Opioid Peptides **2a**−**c**

	Ac-[Ala^2,D-Leu^5]-Enk-NH$_2$ **2a**	Ac-[D-Ala^2,Leu^5]-Enk-NH$_2$ **2b**	Ac-[Ala^2,Leu^5]-Enk-NH$_2$ **2c**
cLogP	0.7	0.7	0.7
molecular surface area (Å^2)	493	491	544
polar surface area (Å^2)	253	257	285
polar surface area (% of the total molecular surface area)	51	52	52

and/or the oxygen of the oxymethyl group.[8] Accordingly, the energy-minimized average structure of **1a** obtained by MD simulations shows one hydrogen bond between the NH of Gly and the oxygen of the phenol group.

In summary, both the spectroscopic and MD simulation studies suggest differences in solution structures among cyclic prodrugs **1a**−**d**. The apparent increase in the number of intramolecular hydrogen bonds and the restricted conformational flexibility of cyclic prodrugs **1b**−**d** compared to **1a** would suggest that there may be differences in their physicochemical properties and thus differences in their cell membrane permeation characteristics.

Physicochemical Properties. Certain physicochemical properties are typically predictive of the intrinsic cell membrane permeation of a molecule via the transcellular pathway. For instance, as the molecular surface area or polar surface area of a transcellular permeant increases, its cell membrane permeation will decrease.[4,32−34] In contrast, the relationship between cLogP and cell membrane permeation is nonlinear, i.e., the permeability decreases and plateaus at both low (e.g., negative) and high cLogP values.[35]

To determine these relationships for the cyclic prodrugs (**1a**−**d**) and the capped peptides (**2a**−**c**), their physicochemical parameters were calculated using Sybyl 6.9; the results are

Table 4. Apparent Permeability Coefficients (P_{app}) of Cyclic Prodrugs **1a** and **1b** (A) and **1c** and **1d** (B) across Caco-2 Cell Monolayers in the Presence and Absence of Known Inhibitors of P-gp and MRP2

A

	P_{app}, cm/s ($\times 10^7$)[a]					
	OMCA-DADLE **1a**			OMCA-[Ala^2,D-Leu^5]-Enk **1b**		
	AP-to-BL	BL-to-AP	ratio	AP-to-BL	BL-to-AP	ratio
w/o inhibitor	0.80 ± 0.1	53.6 ± 10.9	67	0.61 ± 0.1	27.4 ± 0.5	45
GF120918 (2 μM)	2.5 ± 0.2	33.1 ± 1.0	13	1.3 ± 0.4	7.0 ± 1.2	5.4
GF120918 (10 μM)	5.1 ± 0.01	14.2 ± 1.1	2.8	6.4 ± 2.9	13.4 ± 1.5	2.1
MK 571 (50 μM)	8.3 ± 1.9	40.8 ± 1.0	4.9	10.5 ± 1.3	30.0 ± 3.6	2.9
CsA (20 μM)	2.0 ± 0.5	12.1 ± 1.8	6.1	1.4 ± 0.2	8.6 ± 0.9	6.1

B

	P_{app}, cm/s ($\times 10^7$)[a]					
	OMCA-[D-Ala^2,Leu^5]-Enk **1c**			OMCA-[Ala^2,Leu^5]-Enk **1d**		
	AP-to-BL	BL-to-AP	ratio	AP-to-BL	BL-to-AP	ratio
w/o inhibitor	0.29 ± 0.05	28.1 ± 2.9	97	0.51 ± 0.05	18.1 ± 2.8	35
GF120918 (2 μM)	2.0 ± 0.3	10.0 ± 0.9	5.0	2.4 ± 0.5	5.9 ± 1.4	2.5
GF120918 (10 μM)	4.0 ± 0.9	9.0 ± 0.9	2.3	4.8 ± 0.3	9.0 ± 1.3	1.9
MK 571 (50 μM)	5.1 ± 0.4	14.1 ± 1.9	2.8	10.4 ± 1.9	34.5 ± 4.0	3.3
CsA (20 μM)	0.96 ± 0.2	13.2 ± 1.5	14	0.94 ± 0.4	10.9 ± 2.2	12

[a] P_{app} values are presented as mean ± SD ($n = 3$).

shown in Tables 2 and 3, respectively. Cyclic prodrugs **1a**−**d** are more lipophilic than the capped peptides **2a**−**c** as indicated by their higher cLogP values (5.4 and 0.7, respectively). These higher cLogP values for the cyclic prodrugs are not unexpected because of the lipophilic nature of the promoiety.[8,36] Additionally, cyclization of the peptides positions the hydrophobic side chains so that the polar backbone is shielded, which could have a substantial effect on lipophilicity. Because Sybyl accounts only for the two-dimensional (2D) structure, the calculated cLogP values for cyclic prodrugs **1a**−**d** are identical. A similar observation was made for the capped peptides (**2a**−**c**). However, based on high-performance liquid chromatography (HPLC) retention times, differences in polarity were noted (OMCA-[Ala^2,Leu^5]-Enk (most polar) > OMCA-[D-Ala^2,Leu^5]-Enk > OMCA-[Ala^2,D-Leu^5]-Enk > OMCA-DADLE). Cyclic prodrugs **1a**−**d** and capped peptides **2a**−**c** have different molecular surface areas ranging from 560 to 650 A^2 for the cyclic prodrugs and from 491 to 574 A^2 for the capped peptides. Likewise, the polar surface areas varied from 139 to 170 A^2 and from 253 to 323 A^2 for the cyclic prodrugs and capped peptides, respectively.

The data shown in Tables 2 and 3 clearly show the impact that cyclization of a peptide has on its physicochemical properties. While the molecular surface areas of cyclic prodrugs **1a**−**d** are perhaps slightly greater than those of the capped linear peptides **2a**−**c**, the polar surface areas of **1a**−**d** are significantly lower than those of **2a**−**c**. Significant differences in the cLogP values were also observed, i.e., the cLogP values for cyclic prodrugs **1a**−**d** are 5.4 vs 0.7 for the capped linear peptides. These differences in cLogP and polar surface area would suggest that the intrinsic permeation of cyclic prodrugs **1a**−**d** should be significantly greater than the intrinsic permeation of the capped linear peptides **2a**−**c**.

Transport Studies. Previously, our laboratory had shown that OMCA-DADLE (**1a**) was a substrate for efflux transporters (e.g., P-gp, MRP2),[9,10,13] which significantly limited its ability to permeate cell membranes. In an attempt to modify this efflux transporter substrate activity and thus alter its cell permeation characteristics, we prepared analogues of DADLE that had changes in the chirality of Ala and Leu in the 2 and 5 positions, respectively, of this opioid peptide.

The Caco-2 cell permeation characteristics of OMCA-DADLE (**1a**), OMCA-(Ala^2,D-Leu^5)-Enk (**1b**), OMCA-(D-Ala^2,-Leu^5)-Enk (**1c**), and OMCA-(Ala^2,Leu^5)-Enk (**1d**) across Caco-2 cell monolayers are provided in Table 4. Like OMCA-DADLE (**1a**), the analogues **1b**−**d** all exhibited low Caco-2 permeation. In all cases, the BL-to-AP P_{app} values were significantly greater (35 to 97 times) than the AP-to-BL P_{app} values, suggesting that these diastereomers are all substrates for efflux transporters in Caco-2 cells. Since MDR1 inhibitors (e.g., GF120918 ($C_{34}H_{33}N_3O_5$, *N*-(4-[2-(1,2,3,4-tetrahydro-6,7-dimethoxy-2-isoquinolyl)ethyl]phenyl)-9,10-dihydro-5-methoxy-9-oxo-4-acridine carboxamide), cyclosporin A (CsA, $C_{62}H_{111}N_{11}O_{12}$, 3-ethyl-6-(1-hydroxy-2-methyl-pent-3-enyl)-12,15,24,30-tetraisobutyl-9,27-diisopropyl-1,4,7,10,13,16,18,21,25,31-decamethyl-1,4,7,10,13,16,19,22,25,28,31-undecaazacyclotritriacontan-2,5,8,11,14,17,20,23,26,29,32-undecaone)) and MRP2 inhibitors (e.g., CsA, MK 571 ($C_{26}H_{27}ClN_2O_3S_2$, 3-{3-[2-(7-chloroquinolin-2-yl)-vinyl]-phenyl}-3-(2-dimethylcarbamoyl-ethylsulfanylmethylsulfanyl)-propionic acid)) increase the AP-to-BL P_{app} values and, thus, decrease the $P_{app\ BL-to-AP}/P_{app\ P-to-BL}$ ratios, the diastereomers **1b**−**d** appear to be substrates for MDR1 and MRP2. These data are very similar to the results observed with OMCA-DADLE (**1a**).[10]

The cell permeation data suggest that despite differences in the solution conformations, cyclic prodrugs **1a**−**d** must all present a structural feature(s) that is recognized by these efflux transporters. One structural feature that has been shown to be essential for substrate recognition by P-gp is at least one so-called type I or type II unit. These type I and type II units are entirely based on the particular arrangement of electron donor groups and spatial separation distances (2.2 to 2.8 Å or 4.0 to 5.2 Å) in the molecule. These optimally arranged polar groups are then recognized by P-gp.[18,19,37] Since these diastereomers all exhibit potential type I and type II units as determined computationally (data not shown), it is not unexpected that they would exhibit substrate activity for this efflux transporter.

On the basis of the differences in the preferred conformation of cyclic prodrugs **1a**−**d** as determined by NMR and MD simulation, particularly the differences in molecular hydrogen bonding interactions, one might expect to see differences in the intrinsic permeabilities of these diastereomers. Unfortunately, as shown in Table 4, complete inhibition of their efflux in Caco-2 cells was never achieved; thus, we were unable to determine accurately the intrinsic permeabilities of **1a**−**d**.

Table 5. Apparent Permeability Coefficients (P_{app}) of the Capped Linear Opioid **2a**−**c** Peptides across Caco-2 Cell Monolayers in the Presence and Absence of Known Inhibitors of P-gp and MRP2

	P_{app}, cm/ s ($\times 10^7$)[a]								
	Ac-[Ala^2,D-Leu^5]-Enk-NH$_2$ **2a**			Ac-[D-Ala^2,Leu^5]-Enk-NH$_2$ **2b**			Ac-[Ala^2,Leu^5]-Enk-NH$_2$ **2c**		
	AP-to-BL	BL-to-AP	ratio	AP-to-BL	BL-to-AP	ratio	AP-to-BL	BL-to-AP	ratio
w/o inhibitor	0.17 ± 0.03	0.42 ± 0.09	2.5	0.27 ± 0.08	0.76 ± 0.08	2.8	0.22 ± 0.03	0.58 ± 0.26	2.6
GF120918 (10 μM)	0.38 ± 0.01	0.39 ± 0.07	1.0	0.54 ± 0.13	0.57 ± 0.02	1.1	0.14 ± 0.01	0.29 ± 0.12	2.1
MK 571 (50 μM)	0.29 ± 0.06	1.1 ± 0.8	3.8	0.68 ± 0.13	0.73 ± 0.16	1.1	0.64 ± 0.06	1.3 ± 0.1	2.0
CsA (20 μM)	0.20 ± 0.01	0.23 ± 0.06	1.2	1.1 ± 0.2	2.7 ± 1.4	2.4	0.21 ± 0.01	0.37 ± 0.01	1.8

[a] P_{app} values are presented as mean ± SD ($n = 3$).

In an attempt to resolve the importance of the OMCA linker in cyclic prodrugs **1a**−**d** as a determinant for efflux transporter substrate activity, we assessed the Caco-2 cell permeation characteristics of the capped linear opioid peptides **2a**−**c**. As shown in Table 5, all of these capped linear peptides exhibited very low permeation across Caco-2 cell monolayers. Unlike those of cyclic prodrugs **1a**−**d**, the low AP-to-BL P_{app} values observed for the capped linear peptides **2a**−**c** are not the result of extensive efflux. Instead, as predicted by their low cLogP values and high polar surface areas, these capped linear peptides appear to have low intrinsic cell permeation via the transcellular pathway. While it was impossible to determine the intrinsic permeability of cyclic prodrugs **1a**−**d**, they appear (by comparing their P_{app} values determined in the presence of 10 μM GF120918 to the corresponding P_{app} values of the capped peptides) qualitatively to be at least 7-fold more able to permeate than the capped linear peptides **2a**−**c**.

The poor substrate activity of the capped linear peptides **2a**−**c** for efflux transporters in Caco-2 cells would suggest that the OMCA linker either makes cyclic prodrugs **1a**−**d** sufficiently lipophilic to gain access to efflux transporters in the lipid bilayer and/or the cyclization creates solution structures (e.g., β-turns) that are recognized by the efflux transporters, making these cyclic prodrugs candidates for efflux.

Conclusion

We have demonstrated that changes in the chirality of amino acids in the peptide portion of cyclic prodrugs can have a tremendous effect on the solution structure. However, despite different solution conformations and physicochemical properties, all molecules exhibited substrate activity for efflux transporters that could severely limit their oral bioavailability and penetration to the brain in vivo. This substrate activity for efflux transporters is most likely due to the chemical linker used to prepare the cyclic prodrugs and/or its effect on the solution structures of these molecules.

Experimental Section

Materials. L-Glutamine (200 mM (100×)), penicillin (10000 U/mL), streptomycin (10000 μg/mL), fetal bovine serum (FBS), and nonessential amino acids (10 mM (100×) in 85% saline) were obtained from Gibco BRL, Life Technologies (Grand Island, NY). Dulbecco's modified Eagle medium (DMEM) and trypsin/ethylenediaminetetraacetic acid (EDTA) solution (0.25% and 0.02%, respectively, in Ca^{2+}- and Mg^{2+}-free Hank's balanced salt solution (HBSS)) were purchased from JRH Bioscience (Lenexa, KS). D-[1-^{14}C]-Mannitol (specific activity 2.15 GBq/mmol) was purchased from Amersham Biosciences (Uppsala, Sweden). Polyester membranes (Transwell, 0.4 μm pore size, 24 mm diameter) were obtained from Fisher Scientific (Pittsburgh, PA). MK 571 was ordered from Biomol Research Laboratories, Inc. (Plymouth Meeting, PA). GF120918 was donated by Dr. Kenneth Brouwer (GlaxoSmithKline, Research Triangle Park, NC). OMCA-DADLE (**1a**) was synthesized in our laboratory following procedures described elsewhere.[8] All other chemicals and solvents were purchased from Aldrich Chemical Co. (Milwaukee, WI), Sigma Chemical Co. (St. Louis, MO), Fluka Chemical Corp. (Milwaukee, WI), Bachem Bioscience, Inc. (King of Prussia, PA), Fisher Scientific (Pittsburgh, PA), and Novabiochem (La Jolla, CA) and used as received.

Synthesis. Cyclic Prodrugs. The syntheses of cyclic prodrugs **1b**−**d** (Figure 1) were carried out by following standard solution-phase procedures described previously by our laboratory.[8] Standard Boc-amino acid solution-phase chemistry was employed to synthesize the tetrapeptide fragment with the appropriate amino acids. Unless specifically designated, amino acids employed were L-configurations. The structural identity and purity of the cyclic prodrugs were confirmed by ^{1}H NMR, FAB-MS, and analytical HPLC.

OMCA-[Ala^2,D-Leu^5]-Enk (1b). ^{1}H NMR (500 MHz, DMSO-d_6) δ 0.72 (d, 3H, $J = 5.9$ Hz), 0.78 (d, 3H, $J = 6.0$ Hz), 1.18 (d, 3H, $J = 7.0$ Hz), 1.34 (m, 2H), 1.48 (m, 1H), 2.69 (m, 2H), 2.88 (m, 2H), 3.18 (m, 1H), 3.76 (m, 1H), 4.03 (m, 1H), 4.10 (m, 1H), 4.31 (m, 1H), 4.52 (m, 1H), 5.72 (dd, 2H, $J_1 = J_2 = 6.6$ Hz), 6.05 (d, 1H, $J = 12.6$), 6.71 (d, 2H, $J = 8.5$ Hz), 6.91 (m, 1H), 6.80−7.28 (m, 12H), 7.42 (d, 1H, $J = 7.7$), 7.71 (d, 1H, $J = 8.4$), 7.94 (d, 1H, $J = 7.9$), 8.13 (m, 1H), 8.29 (d, 1H, $J = 8.3$). FAB-MS: m/z 728.3 (M + 1).

OMCA-[D-Ala^2,Leu^5]-Enk (1c). ^{1}H NMR (500 MHz, DMSO-d_6) δ 0.82 (d, 3H, $J = 6.1$ Hz), 0.87 (d, 3H, $J = 6.1$ Hz), 1.09 (d, 3H, $J = 7.2$ Hz), 1.54 (m, 3H), 2.85 (m, 3H), 3.58 (m, 2H), 3.98 (m, 1H), 4.23 (m, 2H), 4.39 (m, 2H), 5.65 (d, 1H, $J = 6.6$ Hz), 5.78 (d, 1H, $J = 6.6$ Hz), 6.04 (d, 1H, $J = 12.5$ Hz), 6.70 (d, 2H, $J = 8.5$ Hz), 7.00−7.34 (m, 12 H), 7.37 (d, 1H, $J = 7.8$), 7.49 (d, 1H, $J = 8.5$), 8.22 (d, 1H, $J = 8.3$), 8.33 (d, 1H, $J = 6.6$), 8.49 (d, 1H, $J = 5.9$). FAB-MS: m/z 728.5 (M + 1).

OMCA-[Ala^2,Leu^5]-Enk (1d). ^{1}H NMR (500 MHz, DMSO-d_6) δ 0.81 (d, 3H, $J = 5.8$ Hz), 0.88 (d, 3H, $J = 5.9$ Hz), 1.18 (d, 3H, $J = 6.9$ Hz), 1.53 (m, 2H), 1.65 (m, 1H), 2.55 (m, 2H), 2.81 (m, 2H), 3.10 (dd, 1H, $J_1 = J_2 = 4.7$ Hz), 3.77 (m, 1H), 3.93 (m, 1H), 4.13 (m, 1H), 4.42 (m, 2H), 5.76 (d, 1H, $J = 6.7$), 5.81 (d, 1H, $J = 6.8$ Hz), 5.97 (d, 1H, $J = 12.6$), 6.68 (d, 2H, $J = 8.4$ Hz), 6.81 (m, 2H), 7.01 (d, 2H, $J = 8.4$), 7.18 (m, 8H), 7.72 (d, 1H, $J = 8.7$), 8.19 (s, 1H), 8.35 (d, 2H, $J = 6.6$), 9.20 (s, 1H). FAB-MS: m/z 728.3 (M + 1).

Capped Peptides—Method A (Scheme 1). Method A was used to synthesize the N-acetylated, C-amidated derivatives of [Ala^2,D-Leu^5]-Enk (**2a**) and [Ala^2,Leu^5]-Enk (**2c**). Final products were all purified by column chromatography and characterized by ^{1}H NMR and FAB-MS.

NH$_2$-Tyr-Ala-Gly-Phe-OAll. Following a previously published procedure,[8] Boc-Tyr-Ala-Gly-Phe-OAll (**3**) (0.710 g, 1.0 mmol) was dissolved in ethyl acetate (30 mL) and cooled to 0 °C. HCl (gas) was bubbled into the solution for 10 min, and the solution was then stirred for an additional 20 min. The ethyl acetate was removed by rotary evaporation to give a white solid in quantitative yield. This product was used in the next step without purification. $R_f = 0.1$ (100% ethyl acetate).[8]

Ac-Tyr(OAc)Ala-Gly-Phe-OAll (4). NH$_2$-Tyr-Ala-Gly-Phe-OAll (610 mg, 1.0 mmol) was dissolved in 10 mL of dioxane: water (1:1, 10 mL) and acetic anhydride (3 mL). The solution was stirred for 4 h at room temperature. The solvents were removed in vacuo to give a white solid, which was used in the next step without

purification. $R_f = 0.4$ ($CHCl_3/CH_3OH$, 10:1). ^1H NMR (400 MHz, CD_3OD) δ 1.3 (d, 3H, $J = 7.2$ Hz), 1.90 (s, 3H), 2.23 (s, 3H), 2.90 (dd, 1H, $J_1 = 8.7$ Hz, $J_2 = 14.0$ Hz), 3.30−3.34 (m, 3H), 3.75 (d, 1H, $J = 17.0$ Hz), 3.90 (d, 1H, $J = 17.0$ Hz), 4.25 (q, 1H, $J = 7.1$ Hz), 4.54−4.60 (m, 3H), 4.68 (dd, 1H, $J_1 = 6.1$ Hz, $J_2 = 8.2$ Hz), 5.17 (dd, 1H, $J_1 = 1.0$, $J_2 = 10.8$ Hz), 5.26 (dd, 1H, $J_1 = 1.5$ Hz, $J_2 = 17.2$ Hz), 5.79−5.87 (m, 1H), 6.99 (d, 2H, $J = 8.5$ Hz), 7.18−7.29 (m, 7 H).

Ac-Tyr-Ala-Gly-Phe-OH (5). Ac-Tyr(OAc)Ala-Gly-Phe-OAll (**4**) was dissolved in CH_3OH (75 mL), and aqueous LiOH (250 mg dissolved into 25 mL of water) was added. LiOH is able to deprotect the C-terminus and the *O*-acetyl ester of tyrosine.[25] After the reaction mixture was stirred at room temperature for 24 h, the CH_3OH was removed by rotary evaporation. The aqueous solution was then acidified by 2 N HCl and dried in vacuo. The resulting white solid was suspended in CH_3OH (50 mL) and filtered, and the CH_3OH was evaporated to give a white solid containing the N-acetylated peptide, which was used in the next step without purification. $R_f = 0.4$ ($CHCl_3/CH_3OH$, 1:1). ^1H NMR (400 MHz, CD_3OD) δ 1.34 (d, 3H, $J = 7.1$ Hz), 1.95 (s, 3H), 2.85 (dd, 1H, $J_1 = 8.4$ Hz, $J_2 = 13.9$ Hz), 3.01−3.09 (m, 2H), 3.19 (dd, 1H, $J_1 = 5.1$ Hz, $J_2 = 6.3$ Hz), 3.74 (d, 1H, $J = 13.2$ Hz), 3.90 (d, 1H, $J = 16.9$ Hz), 4.27 (q, 1H, $J = 7.3$), 4.50 (t, 1H, $J = 7.3$ Hz), 4.62 (dd, 1H, $J_1 = 5.0$ Hz, $J_2 = 8.1$ Hz), 6.7 (d, 2H, $J = 8.5$ Hz), 7.08 (d, 2H, $J = 8.4$ Hz), 7.18−7.28 (m, 5H).

Ac-Tyr-Ala-Gly-Phe-Leu-NH_2 (2c). To Ac-Tyr-Ala-Gly-Phe-OH (**5**) (1.2 mmol) in dimethylformamide (DMF) (5 mL) was added dry tetrahydrofuran (THF) (15 mL); the solution was cooled over ice. 1-(3-Dimethylaminopropyl)-3-ethylcarbodiimide hydrochloride (EDC·HCl) (242 mg, 1.26 mmol) and 1-hydroxybenzotriazole (HOBt) (17 mg, 1.26 mmol) were added, and the solution was stirred for 30 min. Triethylamine (TEA) (256 mg, 352 μL, 2.53 mmol), 4-dimethylamino pyridine (DMAP) (15 mg, 0.126 mmol), and Leu-NH_2 (164 mg, 1.26 mmol) were added. The reaction mixture was allowed to warm to room temperature and stirred under N_2. After the mixture was stirred overnight, the solvent was reduced by rotary evaporation and dried in vacuo. The residue was purified by silica gel column chromatography eluting with $CHCl_3/CH_3OH$ (9:1 followed by 3:1 followed by 1:1). Note: DMAP elutes in 9:1 $CHCl_3/CH_3OH$ and the peptide elutes with increasing amounts of CH_3OH. This purification yielded a white solid (4.0 mg, 1.2% yield). Contaminants (HOBt and TEA) remaining after purification were removed by rinsing the white solid with minimal amounts of ice-cold water until NMR spectroscopy showed that the peptide was pure. $R_f = 0.6$ ($CHCl_3/CH_3OH$, 8:2). ^1H NMR (400 MHz, CD_3OD) δ 0.91 (d, 3H, $J = 6.0$ Hz), 0.95 (d, 3H, $J = 0.9$ Hz), 1.33 (d, 3H, $J = 7.2$ Hz), 1.70−1.80 (m, 3H), 1.95 (s, 3H), 2.86 (dd, 1H, $J_1 = 8.3$, $J_2 = 13.8$ Hz), 3.00−3.06 (m, 2H), 3.22 (dd, 1H, $J_1 = 5.5$ Hz, $J_2 = 14.0$ Hz), 3.69 (d, 1H, $J = 16.7$ Hz), 3.83 (d, 1H, $J = 16.8$ Hz), 4.22 (q, 1H, $J = 7.1$ Hz), 4.35 (dd, 1H, $J_1 = 4.3$ Hz, $J_2 = 10.3$ Hz), 4.55 (t, 1H, $J = 8.1$ Hz), 4.62 (dd, 1H, $J_1 = 4.4$ Hz, $J_2 = 8.8$ Hz), 6.70 (d, 2H, $J = 8.5$ Hz), 7.06 (d, 2H, $J = 8.6$ Hz), 7.21−7.31 (m, 5H). FAB-MS: m/z 611.4 (M + 1).

Ac-Tyr-Ala-Gly-Phe-D-Leu-NH_2 (2a). The D-Leu analogue (**2a**) was synthesized as described above by coupling Ac-Tyr-Ala-Gly-Phe-OH (**5**) to D-Leu-NH_2. $R_f = 0.6$ ($CHCl_3/CH_3OH$, 8:2). ^1H NMR (400 MHz, CD_3OD) δ 0.73 (d, 3H, $J = 6.4$ Hz), 0.79 (d, 3H, $J = 6.6$ Hz), 1.36 (d, 3H, $J = 7.2$ Hz), 1.40−1.64 (m, 3H), 1.94 (s, 3H), 2.87 (dd, 1H, $J_1 = 8.2$ Hz, $J_2 = 13.9$ Hz), 3.00−3.09 (m, 3H), 3.75 (d, 1H, $J = 16.9$ Hz), 3.87 (d, 1H, $J = 16.9$ Hz), 4.14−4.23 (m, 2H), 4.48−4.55 (m, 2H), 6.73 (d, 2H, $J = 6.7$ Hz), 7.07 (d, 2H, $J = 8.5$ Hz), 7.23−7.30 (m, 5H). FAB-MS: m/z 611.4 (M + 1).

Capped Peptides—Method B (Scheme 1). Method B was used to synthesize the N-acetylated, C-amidated derivatives of [D-Ala^2,-Leu^5]-Enk (**2b**). The final product was purified by column chromatography and characterized by ^1H NMR and FAB-MS.

Boc-Tyr-D-Ala-Gly-Phe-OH (6). Boc-Tyr-D-Ala-Gly-Phe-OAll (**3**) (1.5 g) was dissolved in CH_3OH (160 mL), and aqueous LiOH (530 mg LiOH in 53 mL of water) was added.[25] After the reaction mixture was stirred at room temperature for 24 h, the CH_3OH was removed by rotary evaporation. The aqueous solution was then neutralized (pH 4−5 as monitored by pH paper) with TFA and dried in vacuo. The resulting white solid was used in the next step without purification. $R_f = 0.4$ ($CHCl_3/CH_3OH$, 1:1). ^1H NMR (400 MHz, CD_3OD) δ 1.22 (d, 3H, $J = 7.2$ Hz), 1.41 (s, 9H), 2.84 (dd, 1H, $J_1 = 7.3$, $J_2 = 13.5$ Hz), 2.94 (dd, 1H, $J = 7.8$, $J_2 = 10.6$ Hz), 3.05 (dd, 1H, $J_1 = 7.9$ Hz, $J_2 = 13.6$ Hz), 3.24 (dd, 1H, $J_1 = 4.3$ Hz, $J_2 = 13.7$ Hz), 3.78 (d, 1H, $J = 16.7$ Hz), 3.85 (d, 1H, $J = 16.9$ Hz), 4.16 (t, 1H, $J = 7.5$ Hz), 4.27 (dd, 1H, $J_1 = J_2 = 7.1$ Hz), 4.56 (t, 1H, $J = 7.2$ Hz), 6.73 (d, 2H, $J = 8.3$ Hz), 7.06 (d, 2H, $J = 8.3$ Hz), 7.19−7.29 (m, 5H).

Boc-Tyr-D-Ala-Gly-Phe-Leu-NH_2 (7). Boc-Tyr-D-Ala-Gly-Phe-OH (**6**) (750 mg, 1.25 mmol) was dissolved in DMF (5 mL) followed by dry THF (10 mL) and cooled to 0 °C. EDC·HCl (251 mg, 1.31 mmol) and HOBt (177 mg, 1.31 mmol) were added and the suspension stirred for 30 min. TEA (273 mg, 376 μL, 2.7 mmol), DMAP (16 mg, 0.131 mmol), and Leu-NH_2 (171 mg, 1.31 mmol) were added, and the reaction mixture was allowed to warm to room temperature and was stirred under N_2. After being stirred overnight, the suspension was reduced by rotary evaporation and dried in vacuo. The residue was purified by silica gel column chromatography with $CHCl_3/CH_3OH$ (9:1, followed by 3:1, followed by 1:1). Note: DMAP eluted in 9:1 $CHCl_3/CH_3OH$. Increasing amounts of CH_3OH lead to elution of the peptide. $R_f = 0.6$ ($CHCl_3/CH_3OH$, 8:2). Contaminants (HOBt and TEA) were removed by rinsing the white solid with minimal amounts of ice-cold water until NMR spectroscopy showed that the peptide was pure (183 mg, 22% yield). ^1H NMR (400 MHz, CD_3OD) δ 0.90 (d, 3H, $J = 6.0$ Hz), 0.96 (d, 3H, $J = 6.0$ Hz), 1.22 (d, 3H, $J = 1.22$ Hz), 1.41 (s, 9H), 3.74 (d, 1H, $J = 16.8$ Hz), 3.91 (d, 1H, $J = 16.4$ Hz), 4.17−4.21 (m, 2H), 4.24−4.32 (m, 1H), 4.56 (t, 1H, $J = 7.1$ Hz), 6.73 (d, 2H, $J = 8.4$ Hz), 7.04 (d, 2H, $J = 8.5$ Hz), 7.21−7.32 (m, 5H).

NH_2-Tyr-D-Ala-Gly-Phe-Leu-NH_2 (8). Boc-Tyr-D-Ala-Gly-Phe-Leu-NH_2 (**7**) was dissolved in ethyl acetate (30 mL) cooled to 0 °C. HCl (gas) was bubbled into the solution for 10 min, and then the solution was stirred for an additional 20 min. The ethyl acetate was removed by rotary evaporation to give a white solid in quantitative yield. This product was used in the next step without purification. $R_f = 0.1$ (100% ethyl acetate). ^1H NMR (400 MHz, CD_3OD) δ 0.90 (d, 3H, $J = 7.4$ Hz), 0.95 (d, 3H, $J = 6.3$ Hz), 1.30 (d, 3H, $J = 7.2$ Hz), 3.05 (dd, 2H, $J_1 = 8.0$, $J_2 = 12.4$ Hz), 3.15−3.20 (m, 2H), 3.82 (s, 2H), 4.08 (t, 1H, $J = 7.3$ Hz), 4.22 (dd, 1H, $J_1 = 7.2$ Hz, $J_2 = 14.3$ Hz), 4.25−4.29 (m, 1H), 4.68 (dd, 1H, $J_1 = 5.6$ Hz, $J_2 = 8.2$ Hz), 6.82 (d, 2H, $J = 6.8$ Hz), 7.14 (d, 2H, $J = 8.5$ Hz), 7.25−7.36 (m, 5H).

Ac-Tyr-D-Ala-Gly-Phe-Leu-NH_2 (2b). NH_2-Tyr-D-Ala-Gly-Phe-Leu-NH_2 (**8**) was dissolved in dioxane:water (1:1, 10 mL) and acetic anhydride (3 mL). The solution was stirred for 4 h at room temperature. The solvents were removed in vacuo to give a white solid. This solid was then dissolved in CH_3OH (4 mL), water (2 mL), and saturated bicarbonate (2 mL) and stirred for 1 h in order to remove any O-acylation from the tyrosine residue.[38] The CH_3OH was removed by rotary evaporation. The resulting aqueous solution was neutralized with HCl, and the solvent was removed in vacuo to afford a white solid. $CHCl_3/CH_3OH$ (1:1) was used to redesolve the peptide and the suspension of salts was gravity filtered. After rotary evaporation, the residue was purified by silica gel column chromatography with $CHCl_3/CH_3OH$ (7% CH_3OH followed by 25% CH_3OH, followed by 50% CH_3OH to elute the peptide) (4.3 mg, 2.4% yield). $R_f = 0.55$ ($CHCl_3/CH_3OH$, 8:2). ^1H NMR (400 MHz, CD_3OD) δ 0.89 (d, 3H, $J = 5.9$ Hz), 0.94 (d, 3H, $J = 5.9$ Hz), 1.24 (t, 3H, $J = 7.2$ Hz), 1.59−1.68 (m, 3H), 1.99 (s, 3H), 2.94 (dd, 2H, $J_1 = 4.9$ Hz, $J_2 = 7.4$ Hz), 3.07 (dd, 1H, $J_1 = 8.9$ Hz, $J_2 = 13.9$ Hz), 3.21 (dd, 1H, $J_1 = 5.6$ Hz, $J_2 = 13.9$ Hz), 3.44 (d, 2H, $J = 3.8$ Hz), 4.13 (q, 1H, $J = 7.3$ Hz), 4.34 (t, 1H, $J = 4.8$ Hz), 4.43 (t, 1H, $J = 7.6$ Hz), 4.60 (dd, 1H, $J_1 = 5.7$ Hz, $J_2 = 8.9$ Hz), 6.74 (d, 2H, $J = 8.5$ Hz), 7.06 (d, 2H, $J = 8.5$ Hz), 7.23−7.31 (m, 5H). FAB-MS: m/z 611.1 (M + 1).

NMR Spectroscopy. Cyclic prodrugs **1b−c** (~3.5 mg) were dissolved in DMSO-d_6 containing approximately 20% H_2O (~0.6 mL). One- and two-dimensional NMR data were acquired on a

Varian Inova 600 at 293 K. Coupling constants ($^3J_{HN\alpha}$) were measured from spectra obtained using double quantum filtered correlated spectroscopy (DQF-COSY). HOHAHA and ROESY experiments were performed with a 70 ms and a 300 ms spin−lock time, respectively. On the basis of the intensity of the amide ROE cross-peaks, the nature of the through space interproton interactions were assigned as strong, medium, or weak with upper and lower boundaries of distances of 1.9−2.5, 2.5−3.5, and 3.5−5.0 Å, respectively. Side chain protons were not assigned stereospecifically; hence, ROE restraints for side chains were calculated by considering pseudo atoms.[30] The NMR data were processed using FELIX software (version 95, Biosym Technologies, San Diego, CA) with a final matrix of 1 K × 1 K real datapoints.

MD Simulations. Solution conformations for cyclic prodrugs **1b**−**d** were determined by MD simulations using the 2D NMR data as described previously by our laboratory.[8] Briefly, MD simulations using ROE constraints were carried out on a Silicon Graphics Computer equipped with Insight II molecular modeling software (Release 98.0, Molecular Simulations, Inc., San Diego, CA). From initial MD simulations performed as described previously,[8] four to nine distinct conformational families were obtained. Average structures from each family were then energy-minimized, solvated with a water layer of 8 Å, and subjected to MD simulations at 300 K using ROE constraints. Several conformations were selected for the final analysis using two criteria: (i) that the conformation had an interproton distance error of less than 0.5 Å compared to upper and lower bounds of distances from ROE data; and (ii) that the conformation had angles within 35° of values calculated from $^3J_{NH\alpha}$. These conformations were minimized with solvent molecules using the conjugate gradient method without a cross term until the rms derivation was 0.4 kcal/mol·Å. Final average energy-minimized solution structures were chosen based on energy and their consistency with the NMR data (dihedral angles and ROE distances).

Physicochemical Properties. Molecular surface area, polar surface area, and cLogP estimations were performed on a Silicon Graphics Computer using Sybyl Version 6.9 (Tripos Inc., St. Louis, MO). The three-dimensional (3D) structures of the N-acetylated and C-amidated opioid peptides were built and energy-minimized using Sybyl. The cyclic opioid peptide prodrugs were energy-minimized starting from the imported structures generated as outlined above (see Molecular Dynamics Simulations). All molecules were in their neutral form. The cLogP values were obtained from the Molecular Spreadsheet. The molecular surface areas and polar surface areas were computed utilizing Connolly molecular surfaces. The polar surface area was defined as the sum of the surface areas of oxygen, nitrogen, and hydrogen atoms attached to nitrogen or oxygen atoms.

Cell Culture. Caco-2 cells (passage 18) were obtained from American Type Culture Collection (Rockville, MD). As described previously,[39] cells were grown in a controlled atmosphere of 5% CO_2 and 90% relative humidity at 37 °C in 150 cm^2 culture flasks using a culture medium consisting of DMEM supplemented with 10% heat-inactivated FBS, 1% nonessential amino acids, 100 μg/mL streptomycin, 100 U/mL penicillin, and 1% L-glutamine. When approximately 80% confluent (i.e., 3−5 days), cells were detached from the plastic support by partial digestion using trypsin/EDTA solution and either subcultured in new flasks or seeded in 6-well cell culture plates on polyester membranes (Transwell, 0.4 μm pore size, 24 mm diameter) at a density of 8.0×10^4 cells/cm^2. Caco-2 cells were fed with culture medium the day after seeding and then every other day until transport experiments were performed (apical (AP) volume 1.5 mL; basolateral (BL) volume 2.6 mL). Cells used in this study were between passages 30 and 39.

Transport Studies. For all transport studies, 21 to 28 day-old Caco-2 cell monolayers grown on polyester membranes (Transwell) were used. The integrity of each batch of cells was verified by measuring [^{14}C]-mannitol flux in representative monolayers. Bidirectional transport experiments were conducted ($n = 3$) at 37 °C in a shaking water bath (30 rpm) in the absence and presence of the MDR1 inhibitor GF120918 (2 μM and 10 μM), the MDR1 and MRP2 inhibitor CsA (20 μM), and the MRP inhibitor MK 571 (50 μM). Cell monolayers were washed 3 times with prewarmed HBSS, pH 7.4. Peptide solutions (final concentration 20 μM) prepared in HBSS containing 0.4% DMSO were applied to the donor compartment (AP: 1.5 mL; BL: 2.6 mL). HBSS was added to the receiver compartment and aliquots (donor: 10 μL; receiver: 100 μL) were removed and replaced with prewarmed HBSS at various time intervals up to 160 min. For transport experiments determining the impact of efflux transporters on the cell permeation, GF120918, CsA, or MK 571 was included in HBSS. The samples withdrawn were diluted with HBSS containing 10% (v/v) acetonitrile and immediately frozen and kept at −80 °C until analysis by high-performance liquid chromatography with tandem mass spectrometric detection (LC-MS-MS). Permeability coefficients (P_{app}) of the cyclic and capped peptides were calculated using the following equation:

$$P_{app} = (\Delta Q/\Delta t)/(A \times C_0)$$

where $\Delta Q/\Delta t$ is the linear appearance rate of mass in the receiver solution, A is the cross-sectional area (4.71 cm^2), and C_0 is the initial peptide concentration of the donor compartment at $t = 0$.

Sample Analysis. LC-MS-MS was employed using a Quattro Micro triple quadrupole mass spectrometer (Micromass, Beverly, MA). The LC was conducted using a Waters 2690 HPLC system (Waters, Milford, MA). The analytical column, which was kept at 25 °C, was a Vydac (Hesperia, CA) C_{18} HPLC column (50 × 1.0 mm i.d., 300 Å, Vydac 218TP) with a guard column (5 μm microbore cartridge, Vydac 218GK51). Sample separation was achieved utilizing a linear gradient from 5% to 100% B (mobile phase: A, water with 0.1% FA (v/v); B, acetonitrile with 0.1% FA (v/v)) and a flow rate of 0.2 mL/min. The total run time was 12 min (5 min gradient 5% to 100% B; 2 min 100% B, 1 min reduction of 100% B to 5% B, 4 min equilibration with 5% B). The eluent of the first two minutes and the last 3 min was directed to waste. Samples were recorded by multiple reaction monitoring (cyclic prodrugs: m/z 728.3 > 120.1; capped peptides: m/z 611.0 > 333.9). The MS-MS conditions for the cyclic prodrugs were as follows: capillary voltage 3.20 kV; cone voltage 30 V, source temperature 120 °C; desolvation gas flow 740 L/h; multiplier voltage 650 V; dwell time 0.15 s; inter-channel delay 0.03 s. The MS-MS conditions for the capped peptides were as follows: capillary voltage 4.0 kV; cone voltage 25 V, source temperature 100 °C; desolvation gas flow 740 L/h; multiplier voltage 650 V; dwell time 0.5 s; inter-channel delay 0.03 s. Data acquisition and analysis were performed using Mass Lynx v3.5 and v4.0 software (Micromass). Further information on analytical methods developed in our laboratory for cyclic prodrugs can be found elsewhere.[40]

Acknowledgment. The authors thank Dr. Hui Ouyang for helpful advice and discussions. Financial support was provided by the United States Public Health Service (DA 09315).

Supporting Information Available: MS, HPLC, and NMR data for the cyclic prodrugs **1b**−**d** and the capped peptides **2a**−**c** and constraints used for MD simulations. This material is available free of charge via the Internet at http://pubs.acs.org.

References

(1) Pauletti, G. M.; Gangwar, S.; Siahaan, T. J.; Aubé, J.; Borchardt, R. T. Improvement of oral peptide bioavailability: Peptidomimetics and prodrug strategies. *Adv. Drug Delivery Rev.* **1997**, *27*, 235−256.
(2) Pardridge, W. M. Blood-brain barrier drug targeting: the future of brain drug development. *Mol. Interventions* **2003**, *3*, 90−105, 151.
(3) Veber, D. F.; Johnson, S. R.; Cheng, H. Y.; Smith, B. R.; Ward, K. W.; Kopple, K. D. Molecular properties that influence the oral bioavailability of drug candidates. *J. Med. Chem.* **2002**, *45*, 2615−2623.
(4) Atkinson, F.; Cole, S.; Green, C.; van de Waterbeemd, H. Lipophilicity and other parameters affecting brain penetration. *Curr. Med. Chem.: Cent. Nerv. Syst. Agents* **2002**, *2*, 229−240.
(5) Pauletti, G. M.; Gangwar, S.; Knipp, G. T.; Nerkurkar, M. M.; Okumu, F. W.; Tamura, K.; Siahaan, T. J.; Borchardt, R. T. Structural requirements for intestinal absorption of peptide drugs. *J. Controlled Release* **1996**, *41*, 3−17.

(6) Wacher, V. J.; Silverman, J. A.; Zhang, Y.; Benet, L. Z. Role of P-glycoprotein and cytochrome P450 3A in limiting oral absorption of peptides and peptidomimetics. *J. Pharm. Sci.* **1998**, *87*, 1322−1330.
(7) Borchardt, R. T. Optimizing oral absorption of peptides using prodrug strategies. *J. Controlled Release* **1999**, *62*, 231−238.
(8) Ouyang, H.; Vander Velde, D. G.; Borchardt, R. T.; Siahaan, T. J. Synthesis and conformational analysis of a coumarinic acid-based cyclic prodrug of an opioid peptide with modified sensitivity to esterase-catalyzed bioconversion. *J. Pept. Res.* **2002**, *59*, 183−195.
(9) Yang, J. Z.; Chen, W.; Borchardt, R. T. In vitro stability and in vivo pharmacokinetic studies of a model opioid peptide, H-Tyr-D-Ala-Gly-Phe-D-Leu-OH (DADLE), and its cyclic prodrugs. *J. Pharmacol. Exp. Ther.* **2002**, *303*, 840−848.
(10) Ouyang, H.; Tang, F.; Siahaan, T. J.; Borchardt, R. T. A modified coumarinic acid-based cyclic prodrug of an opioid peptide: its enzymatic and chemical stability and cell permeation characteristics. *Pharm. Res.* **2002**, *19*, 794−801.
(11) Tang, F.; Borchardt, R. T. Characterization of the efflux transporter-(s) responsible for restricting intestinal mucosa permeation of the coumarinic acid-based cyclic prodrug of the opioid peptide DADLE. *Pharm. Res.* **2002**, *19*, 787−793.
(12) Tang, F.; Borchardt, R. T. Characterization of the efflux transporter-(s) responsible for restricting intestinal mucosa permeation of an acyloxyalkoxy-based cyclic prodrug of the opioid peptide DADLE. *Pharm. Res.* **2002**, *19*, 780−786.
(13) Chen, W.; Yang, J. Z.; Andersen, R.; Nielsen, L. H.; Borchardt, R. T. Evaluation of the permeation characteristics of a model opioid peptide, H-Tyr-D-Ala-Gly-Phe-D-Leu-OH (DADLE), and its cyclic prodrugs across the blood-brain barrier using an in situ perfused rat brain model. *J. Pharmacol. Exp. Ther.* **2002**, *303*, 849−857.
(14) Morley, J. S. Structure−activity relationships of enkephalin-like peptides. *Annu. Rev. Pharmacol. Toxicol.* **1980**, *20*, 81−110.
(15) Ling, N. M. S.; Lazarus, L.; Rivier, J.; Guillemin, R. Structure−activity relationships of enkephalin and endorphin analogs. *Pept., Proc. Am. Pept. Symp., 5th* **1977**, 96−99.
(16) Eriksson, L.; Jonsson, J.; Hellberg, S.; Lindgren, F.; Skagerberg, B.; Sjostrom M.; Wold, S. Peptide QSAR on substance P analogues, enkephalins and bradykinins containing L- and D-amino acids. *Acta Chem. Scand.* **1990**, *44*, 50−55.
(17) Bergstrom, C. A.; Strafford, M.; Lazorova, L.; Avdeef, A.; Luthman, K.; Artursson, P. Absorption classification of oral drugs based on molecular surface properties. *J. Med. Chem.* **2003**, *46*, 558−570.
(18) Seelig, A. A general pattern for substrate recognition by P-glycoprotein. *Eur. J. Biochem.* **1998**, *251*, 252−261.
(19) Seelig, A.; Blatter, X. L.; Wohnsland, F. Substrate recognition by P-glycoprotein and the multidrug resistance-associated protein MRP1: a comparison. *Int. J. Clin. Pharmacol. Ther.* **2000**, *38*, 111−121.
(20) Schwab, D.; Fischer, H.; Tabatabaei, A.; Poli, S.; Huwyler, J. Comparison of in vitro P-glycoprotein screening assays: recommendations for their use in drug discovery. *J. Med. Chem.* **2003**, *46*, 1716−1725.
(21) Pajeva, I. K.; Wiese, M. Pharmacophore model of drugs involved in P-glycoprotein multidrug resistance: explanation of structural variety (hypothesis). *J. Med. Chem.* **2002**, *45*, 5671−5686.
(22) Penzotti, J. E.; Lamb, M. L.; Evensen, E.; Grootenhuis, P. D. A computational ensemble pharmacophore model for identifying substrates of P-glycoprotein. *J. Med. Chem.* **2002**, *45*, 1737−1740.
(23) Ekins, S.; Kim, R. B.; Leake, B. F.; Dantzig, A. H.; Schuetz, E. G.; Lan, L. B.; Yasuda, K.; Shepard, R. L.; Winter, M. A.; Schuetz, J. D.; Wikel, J. H.; Wrighton, S. A. Application of three-dimensional quantitative structure−activity relationships of P-glycoprotein inhibitors and substrates. *Mol. Pharmacol.* **2002**, *61*, 974−981.
(24) Österberg, T.; Norinder, U. Theoretical calculation and prediction of P-glycoprotein-interacting drugs using MolSurf parametrization and PLS statistics. *Eur. J. Pharm. Sci.* **2000**, *10*, 295−303.
(25) Reid, R. C.; Kelso, M. J.; Scanlon, M. J.; Fairlie, D. P. Conformationally constrained macrocycles that mimic tripeptide beta-strands in water and aprotic solvents. *J. Am. Chem. Soc.* **2002**, *124*, 5673−5683.
(26) Gudmundsson, O. S.; Jois, S. D.; Vander Velde, D. G.; Siahaan, T. J.; Wang, B.; Borchardt, R. T. The effect of conformation on the membrane permeation of coumarinic acid- and phenylpropionic acid-based cyclic prodrugs of opioid peptides. *J. Pept. Res.* **1999**, *53*, 383−392.
(27) Gudmundsson, O. S.; Vander Velde, D. G.; Jois, S. D.; Bak, A.; Siahaan, T. J.; Borchardt R. T. The effect of conformation of the acyloxyalkoxy-based cyclic prodrugs of opioid peptides on their membrane permeability. *J. Pept. Res.* **1999**, *53*, 403−413.
(28) Conradi, R. A.; Hilgers, A. R.; Ho, N. F.; Burton, P. S. The influence of peptide structure on transport across Caco-2 cells. II. Peptide bond modification which results in improved permeability. *Pharm. Res.* **1992**, *9*, 435−439.
(29) Conradi, R. A.; Hilgers, A. R.; Ho, N. F.; Burton, P. S. The influence of peptide structure on transport across Caco-2 cells. *Pharm. Res.* **1991**, *8*, 1453−1460.
(30) Wüthrich, K. *NMR of Protein and Nucleic Acids*; John Wiley & Sons, Inc.: New York, 1986.
(31) Rose, G. D.; Gierasch, L. M.; Smith, J. A. Turns in peptides and proteins. *Adv. Protein Chem.* **1985**, *37*, 1−109.
(32) Clark, D. E. Rapid calculation of polar molecular surface area and its application to the prediction of transport phenomena. 2. Prediction of blood-brain barrier penetration. *J. Pharm. Sci.* **1999**, *88*, 815−821.
(33) Kelder, J.; Grootenhuis, P. D.; Bayada, D. M.; Delbressine, L. P.; Ploemen, J. P. Polar molecular surface as a dominating determinant for oral absorption and brain penetration of drugs. *Pharm. Res.* **1999**, *16*, 1514−1519.
(34) He, Y. L.; Murby, S.; Gifford, L.; Collett, A.; Warhurst, G. et al. Oral absorption of D-oligopeptides in rats via the paracellular route. *Pharm. Res.* **1996**, *13*, 1673−1678.
(35) Wils, P.; Warnery, A.; Phung-Ba, V.; Legrain, S.; Scherman, D. High lipophilicity decreases drug transport across intestinal epithelial cells. *J. Pharmacol. Exp. Ther.* **1994**, *269*, 654−658.
(36) Lipinski, C. A. Drug-like properties and the causes of poor solubility and poor permeability. *J. Pharmacol. Toxicol. Methods* **2000**, *44*, 235−249.
(37) Seelig, A. How does P-glycoprotein recognize its substrates? *Int. J. Clin. Pharmacol. Ther.* **1998**, *36*, 50−54.
(38) Büchi, G.; Weinreb, S. M. Total syntheses of aflatoxins M1 and G1 and an improved synthesis of aflatoxin B1. *J. Am. Chem. Soc.* **1971**, *93*, 746−752.
(39) Gao, J.; Hugger, E. D.; Beck-Westermeyer, M. S.; Borchardt, R. T. Protocols in the application of Caco-2 cells in measuring permeability coefficient of drugs. *Current Protocols in Pharmacology*; John Wiley and Sons: New York, 2000; pp 1−23.
(40) Yang, J. Z.; Bastian, K. C.; Moore, R. D.; Stobaugh, J. F.; Borchardt, R. T. Quantitative analysis of a model opioid peptide and its cyclic prodrugs in rat plasma using high-performance liquid chromatography with fluorescence and tandem mass spectrometric detection. *J. Chromatogr. B Anal. Technol. Biomed. Life Sci.* **2002**, *780*, 269−281.

JM050277F